Heat and Mass Transfer 39 (2003) 561–569
DOI 10.1007/s00231-002-0339-2

Simultaneous heat and mass transfer by natural convection from a plate embedded in a porous medium with thermal dispersion effects

Ali J. Chamkha, Mir Mujtaba A. Quadri

Abstract The problem of steady, laminar, simultaneous heat and mass transfer by natural convection flow over a vertical permeable plate embedded in a uniform porous medium in the presence of inertia and thermal dispersion effects is investigated for the case of linear variations of both the wall temperature and concentration with the distance along the plate. Appropriate transformations are employed to transform the governing differential equations to a non-similar form. The transformed equations are solved numerically by an efficient implicit, iterative, finite-difference scheme. The obtained results are checked against previously published work on special cases of the problem and are found to be in good agreement. A parametric study illustrating the influence of the porous medium effects, heat generation or absorption, wall suction or injection, concentration to thermal buoyancy ratio, thermal dispersion parameter, and the Schmidt number on the fluid velocity, temperature and concentration as well as the skin-friction coefficient and the Nusselt and Sherwood numbers is conducted. The results of this parametric study are shown graphically and the physical aspects of the problem are highlighted and discussed.

Nomenclature

A, B	Constants for wall temperature and concentration, respectively
C	Concentration at any point in the flow field
C_f	Local skin friction coefficient defined by Eq. (17)
C_m	Local mass transfer coefficient defined by Eq. (19)
C_q	Local heat transfer coefficient defined by Eq. (18)
C_w	Concentration at the wall
C_∞	Concentration at the free stream
D	Mass diffusivity
Da^*	Inverse Darcy number ($Da^* = \nu/((K(g\beta_T A)^{1/2}))$
F	Inertia coefficient of the porous medium
f	Dimensionless stream function ($f = \psi/((g\beta_T A\nu^2)^{1/4}x)$)
f_o	Dimensionless wall mass transfer coefficient ($f_o = V_w/(g\beta_T A\nu^2)^{1/4}$)
g	Gravitational acceleration
h	Local convective heat transfer coefficient
K	Permeability of the porous medium
k_e	Porous medium effective thermal conductivity
N	Buoyancy ratio ($N=(\beta_C(C_w - C_\infty))/(\beta_T(T_w - T_\infty))$)
Pr	Prandtl number ($Pr = \rho\nu c_p/k_e$)
Q_o	Heat generation or absorption coefficient
S	Porous medium thermal dispersion parameter ($S = \gamma d(g\beta_T A)^{1/2}x/\alpha$)
Sc	Schmidt number ($Sc = \nu/D$)
T	Temperature at any point
T_w	Wall temperature
T_∞	Free stream temperature
u	Tangential or x-component of the Darcian velocity
v	Normal or y-component of the Darcian velocity
V_w	Dimensional wall mass transfer
X	Distance along the plate
Y	Distance normal to the plate

Greek symbols

Γ	Dimensionless porous medium inertia coefficient ($\Gamma = Fc_p/(g\beta_T)$)
α	Molecular thermal diffusivity
α_e	Effective thermal diffusivity of the porous medium
α_d	Thermal diffusivity of the porous medium due to thermal dispersion
β_C	Concentration expansion coefficient
β_T	Thermal expansion coefficient
δ	Dimensionless heat generation or absorption parameter ($\delta = Q_o/(\rho c_p(g\beta_T A)^{1/2})$)
ϕ	Dimensionless concentration ($\phi = (C - C_\infty)/(C_w - C_\infty)$)
γ	Thermal dispersion constant
η	Dimensionless distance normal to the plate ($\eta = (g\beta_T A/\nu^2)^{1/4}y$)
ν	Fluid kinematic viscosity
ψ	Stream function
θ	Dimensionless temperature ($\theta = (T - T_\infty)/(T_w - T_\infty)$)
ρ	Fluid density
ξ	Dimensionless distance along the plate ($\xi = g\beta_T x/c_p$)

Received: 3 April 2001
Published online: 27 May 2003

A.J. Chamkha (✉), M.M.A. Quadri
Department of Mechanical Engineering, Kuwait University,
P.O. Box 5969, Safat, 13060 Kuwait
E-mail: chamkha@kuc01.kuniv.edu.kw

1 Introduction

Simultaneous heat and mass transfer from different geometries embedded in porous media has many engineering and geophysical applications such as geothermal reservoirs, drying of porous solids, thermal insulation,

enhanced oil recovery, packed-bed catalytic reactors, cooling of nuclear reactors, and underground energy transport. Most early studies on porous media have used the Darcy law which is a linear empirical relation between the Darcian velocity and the pressure drop across the porous medium and is limited to relatively slow flows. However, for relatively high velocity flow situations, the Darcy law is inadequate for representing the flow behavior correctly since it does not account for the resulting inertia effects of the porous medium. In this situation, the pressure drop has a quadratic relationship with the volumetric flow rate. The high flow situation is established when the Reynolds number based on the pore size is greater than unity. Vafai and Tien (1981) discussed the importance of inertia effects for high velocity flows in porous media.

Simultaneous heat and mass transfer from a vertical surface embedded in a uniform porous medium was considered by Bejan (1984) based on scale analysis and by Bejan and Khair (1985) based on the boundary-layer similarity method. Lai (1991) investigated coupled heat and mass transfer by mixed convection from an isothermal vertical plate in a porous medium. The effect of wall fluid blowing on the coupled heat and mas transfer boundary-layer flow over a vertical plate was investigated by Lai and Kulacki (1991). Raptis et al. (1981) obtained an anlytical solution for the case of an infinite vertical wall in a porous medium with uniform wall suction effects.

The open literature is rich with investigations dealing with natural convection in porous media. For example, Cheng and Minkowycz (1977) presented similarity solutions for free thermal convection from a vertical plate embedded in a fluid-saturated porous medium for situations where the wall temperature is a power-law function of the distance along the plate. Cheng (1978) provided an extensive review of early work on free convection in porous media with special regard to applications in geothermal systems. Plumb and Huenefeld (1981) considered non-Dracy natural convection from heated surfaces in saturated porous media. Kim and Vafai (1989) analyzed the problem of natural convection about a vertical plate in porous media. Hong et al. (1987) reported on the effects of non-Darcy and non-uniform porosity on the vertical-plate natural convection in porous media. Nield and Bejan (1992) reported an excellent summary of the free convection flow in porous media.

In the presence of a porous medium, a secondary effect on the flow arises as a result of mixing and recirculation of local fluid particles through tortuous paths formed by the porous medium solid particles. This effect is classified as thermal dispersion (see Amiri and Vafai, 1994). Plumb (1983) modeled thermal dispersion effects over a vertical plate as linear increases of a fluid thermal diffusivity with the increases in the tangential flow velocity. In their model, Amiri and Vafai (1994) have shown that the thermal
diffusivity of the fluid is also proportional to the free stream Reynolds number based on the porous medium pore diameter. Other works dealing with thermal dispersion effects in porous media can be found in the papers by Tien (1988) and Cheng and Vortmeyer (1988).

In certain porous media applications such as those involving heat removal from nuclear fuel debris, underground disposal of radioactive waste material, storage of food stuffs, and exothermic chemical reactions and dissociating fluids in packed-bed reactors, the working fluid heat generation (source) or absorption (sink) effects are important. Representative studies dealing with these effects have been reported previously by such authors as Acharya and Goldstein (1985), Vajravelu and Nayfeh (1992) and Chamkha (1996, 1997).

The objective of this paper is to consider simultaneous heat and mass transfer by natural convection from a vertical semi-infinite plate embedded in a fluid-saturated porous medium in the presence of wall suction or injection, heat generation or absorption effects, porous medium inertia and thermal dispersion effects. This will be done for linear variations of both the wall temperature and concentration with the distance along the plate.

2
Problem formulation

Consider steady, laminar, simultaneous heat and mass transfer by natural convection flow over a semi-infinite permeable vertical plate embedded in a fluid-saturated porous medium. Figure 1 shows the schematic diagram and coordinate system of the problem. The fluid is assumed to be Newtonian, heat generating or absorbing and has constant properties except the density in the buoyancy terms of the balance of linear momentum equation. Also, the porosity and permeability of the porous medium are assumed to be constant. The fluid and the porous medium are assumed to be in local thermal equilibrium. Both the wall temperature and concentration are assumed to have linear variations with the plate's vertical distance x. The temperature and the concentration at the plate surface are always greater than their free stream values.

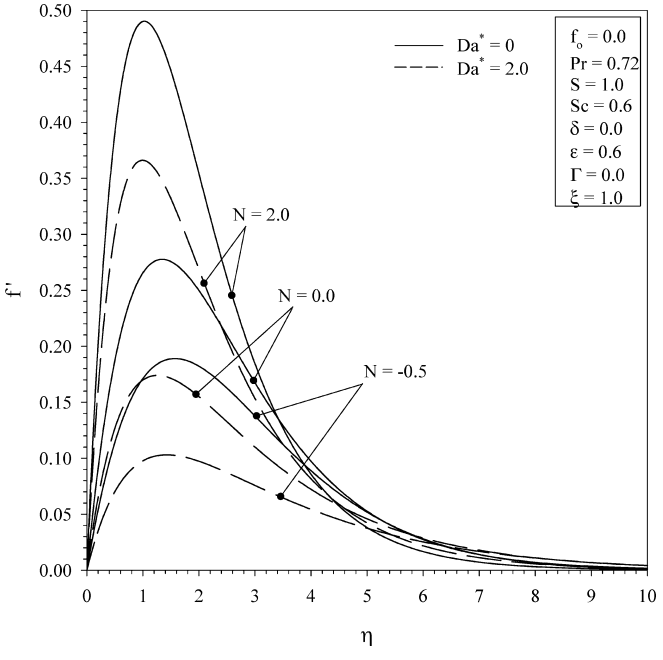

Fig. 1. Effects of Da* and N on the Velocity Profiles

The governing boundary-layer equations which take into account the inertia and thermal dispersion effects of the porous medium within the boundary layer in addition to the Boussinesq approximation may be written as follows:

$$\frac{\partial u}{\partial x}+\frac{\partial v}{\partial y}=0 \tag{1}$$

$$\frac{1}{\varepsilon^2}\left(u\frac{\partial u}{\partial x}+v\frac{\partial u}{\partial y}\right) = \frac{\nu}{\varepsilon}\frac{\partial^2 u}{\partial y^2}+g\beta_T(T-T_\infty)+g\beta_C(C-C_\infty)-\frac{\nu}{K}u-Fu^2 \tag{2}$$

$$u\frac{\partial T}{\partial x}+v\frac{\partial T}{\partial y}=\frac{\partial}{\partial y}\left(\alpha_e\frac{\partial T}{\partial y}\right)+\frac{\nu}{c_p}\left(\frac{\partial u}{\partial y}\right)^2+\frac{Q_o}{\rho c_p}(T-T_\infty) \tag{3}$$

$$u\frac{\partial C}{\partial x}+v\frac{\partial C}{\partial y}=D\frac{\partial^2 C}{\partial y^2} \tag{4}$$

where u, v, T and C are the fluid x-component of the Darcian velocity, y-component of the Darcian velocity, temperature, and concentration, respectively. ρ, ν, c_p, β_T, and β_C are the fluid density, kinematic viscosity, specific heat at constant pressure, coefficient of thermal expansion, and coefficient of concentration expansion, respectively. g, Q_o, and D are the acceleration due to gravity, heat generation (>0) or absorption (<0) coefficient and mass diffusivity, respectively. F, K, α_e and ε are the porous medium inertia coefficient, permeability, effective thermal diffusivity, and porosity, respectively.

The boundary conditions for this problem can be written as

$$y=0: \quad v=V_w, \quad T=T_w(x), \quad C=C_w(x) \tag{5}$$

$$y\to\infty: \quad u\to 0, \quad T\to T_\infty, \quad C\to C_\infty \tag{6}$$

where both the wall temperature T_w and wall concentration C_w vary along the plate according to:

$$T_w-T_\infty=Ax, \quad C_w-C_\infty=Bx \tag{7}$$

In Equations (5) through (7), V_w is the surface mass transfer parameter, T_∞ and C_∞ are the free stream temperature and concentration, respectively and A and B are constants.

In situations of fluid flow and heat transfer in porous media, the effective thermal diffusivity is modeled by Yagi et al. (1964) and later by Plumb (1983) according to

$$\alpha_e=\alpha+\alpha_d \tag{8}$$

where the α and α_d are the molecular and thermal dispersion thermal diffusivities of the fluid and the porous medium, respectively. Yagi et al. (1964) and Plumb (1983) represented α_d as a linear relation of the fluid velocity as follows:

$$\alpha_d=\gamma u d \tag{9}$$

where d is the mean particle diameter and γ is a constant. Gorla et al. (1996) have used the same model.

Defining the dimensional stream function in the usual way such that $u=\frac{\partial\psi}{\partial y}$ and $v=-\frac{\partial\psi}{\partial x}$ and using the following dimensionless variables (El-Hakiem, 2000):

$$\xi=\frac{g\beta_T x}{c_p}, \quad \eta=(g\beta_T A/\nu^2)^{1/4}y, \quad f(\xi,\eta)=\frac{\psi}{(g\beta_T A\nu^2)^{1/4}x}$$
$$\theta(\xi,\eta)=\frac{T-T_\infty}{T_w-T_\infty}, \quad \phi(\xi,\eta)=\frac{C-C_\infty}{C_w-C_\infty} \tag{10}$$

results in the following non-similar equations:

$$\frac{f'''}{\varepsilon}+\frac{ff''}{\varepsilon^2}-Da^*f'-\left(\frac{1}{\varepsilon^2}+\Gamma\xi\right)f'^2+\theta+N\phi = \frac{\xi}{\varepsilon^2}\left(f'\frac{\partial f'}{\partial\xi}-f''\frac{\partial f}{\partial\xi}\right) \tag{11}$$

$$\frac{1}{Pr}(1+Sf')\theta''+\left(\frac{S}{Pr}f''+f\right)\theta'+(\delta-f')\theta = \xi\left(f'\frac{\partial\theta}{\partial\xi}-\theta'\frac{\partial f}{\partial\xi}-(f'')^2\right) \tag{12}$$

$$\frac{1}{Sc}\phi''+f\phi'-f'\phi=\xi\left(f'\frac{\partial\phi}{\partial\xi}-\phi'\frac{\partial f}{\partial\xi}\right) \tag{13}$$

where

$$Da^*=\frac{\nu}{K(g\beta_T A)^{1/2}}, \quad \Gamma=\frac{Fc_p}{g\beta_T}, \quad N=\frac{\beta_C(C_w-C_\infty)}{\beta_T(T_w-T_\infty)}, \quad Pr=\frac{\rho\nu c_p}{k_e}$$
$$Sc=\frac{\nu}{D}, \quad \delta=\frac{Q_o}{\rho c_p(g\beta_T A)^{1/2}}, \quad S=\frac{\gamma d(g\beta_T A)^{1/2}x}{\alpha} \tag{14}$$

are the inverse Darcy number, dimensionless porous medium inertia coefficient, buoyancy ratio, Prandtl number, Schmidt number, dimensionless internal heat generation or absorption parameter, and the porous medium thermal dispersion parameter, respectively.

The dimensionless form of the boundary conditions becomes

$$\eta=0: \quad f+\frac{\partial f}{\partial\xi}=f_o, \quad f'=0, \quad \theta=1, \quad \phi=1 \tag{15}$$

$$\eta\to\infty: \quad f'\to 0, \quad \theta\to 0, \quad \phi\to 0 \tag{16}$$

where $f_o=V_w/(g\beta_T A\nu^2)^{1/4}$ is the dimensionless wall mass transfer coefficient.

The local skin-friction coefficient and local heat and mass transfer coefficients are important physical parameters for this flow and heat transfer situation. These are defined as follows:

$$C_f=\frac{\mu(\partial u/\partial y)_{y=0}}{\rho\nu^{-1/2}(g\beta_T A)^{3/4}c_p(g\beta_T)^{-1}}=\xi f''(\xi,0) \tag{17}$$

$$C_q=\frac{-k_e(\partial T/\partial y)_{y=0}}{k_e\nu^{-1/2}(g\beta_T A)^{1/4}Ac_p(g\beta_T)^{-1}}=-\xi\theta'(\xi,0) \tag{18}$$

$$C_m = \frac{-D(\partial C/\partial y)_{y=0}}{D\nu^{-1/2}(g\beta_T A)^{1/4} B c_p (g\beta_T)^{-1}} = -\xi\phi'(\xi, 0) \qquad (19)$$

3
Numerical method

The implicit finite-difference method discussed by Blottner (1970) has proven to be adequate and accurate for the solution of differential equations similar to Equations (11) through (13). For this reason, it is employed in the present work. These equations have been linearized and then descritized using three-point central difference quotients with variable step sizes in the η direction. A backward difference approximation is used for all first derivatives with respect to ξ. Constant step space sizes in the ξ direction are employed. The resulting equations form a tri-diagonal system of algebraic equations that can be solved at each line of constant ξ by the well-known Thomas algorithm (see Blottner, 1970). Due to the nonlinearities of the equations, an iterative solution is required. For convergence, the maximum absolute error between two successive iterations was taken to be 10^{-7}. A starting step size of 0.001 in the η direction with an increase of 1.0375 times the previous step size and a step size of 0.01 in the ξ direction were found to give accurate results. The total number of points in the ξ and η directions was taken to be 101 and 199, respectively. The accuracy of the aforementioned numerical method was validated by direct comparisons with the numerical results reported earlier by El-Hakiem (2000) for Newtonian fluids. It should be mentioned that El-Hakiem (2000) investigated hydromagnetic free convection flow over a non-isothermal surface in a micropolar fluid. The presence of a porous medium without the inertia effect produces the sma effect as that produced by a magnetic field provided that magnetic. By adding a term simulating the magnetic dissipation effect in the present equations, the results can be compared with those reported by El-Hakiem (2000). Table 1. presents comparisons for the wall slopes of velocity and temperature profiles for various inverse Darcy numbers Da^* and thermal dispersion parameters S. These comparisons show good agreement between the results. The deviations between the results are probably associated with the fact that the results of El-Hakiem (2000) do not appear to approach the free stream values accurately as obvious from the velocity and temperature profiles presented in his paper.

4
Results and discussion

Figures 1 through 3 present representative velocity, temperature and concentration profiles at $\xi = 1$ for various inverse Darcy numbers Da^* and buoyancy ratio values N, respectively. The presence of a porous medium increases the resistance to flow resulting in decreases in the flow velocity and increases in both the temperature and concentration. These behaviors are depicted by the decreases in f' and increases in both θ and ϕ as Da^* increases shown in Figures 1 through 3. Increases in the buoyancy ratio N>0 (aiding flow) have the tendency to increase the buoyancy effects resulting in more induced flow along the surface at the expense of reduced temperature and concentration. On the other hand, opposing flow situations (N<0) produce the opposite effects namely decreases in the flow velocity and increases in the flow temperature and concentration. These behaviors are clear from Figures 1 through 3.

Figures 4 through 6 illustrate the effects of Da^* and N on the distributions of the local skin-friction coefficient C_f, local wall heat transfer coefficient C_q and the local mass transfer coefficient C_m along the surface, respectively. Inspection of Figures 1 through 3 shows that all of the wall slope of velocity and negative wall slopes of temperature and concentration decrease as Da^* increases. This results in decreases in all of C_f, C_q and C_m as Da^* increases. On the other hand, increases in the value of N is predicted to increase the values of C_f, C_q and C_m along the plate except for C_q at large values of N and ξ in the absence of the

Table 1. Comparisons of $f''(\xi, 0)$ and $-\theta'(\xi, 0)$ with El-Hakiem (2000) for various values of Da^*, S and ξ

S	Da^*	ξ	$f''(\xi, 0)$		$-\theta'(\xi, 0)$	
			El-Hakiem (2000)	Present Work	El-Hakiem (2000)	Present Work
0.0	1	0.0	0.61221	0.61457	0.45359	0.45217
		0.5	0.62226	0.62510	0.40463	0.40086
		1.0	0.63272	0.63648	0.35375	0.34433
	4	0.0	0.41708	0.42015	0.34402	0.33209
		0.5	0.42271	0.42639	0.30605	0.29048
		1.0	0.42881	0.43345	0.26540	0.24449
0.2	1	0.0	0.61377	0.61457	0.46411	0.45217
		0.5	0.62385	0.62554	0.41458	0.40643
		1.0	0.63436	0.63733	0.36308	0.35571
	4	0.0	0.41733	0.42015	0.34819	0.33209
		0.5	0.42290	0.42647	0.31018	0.29296
		1.0	0.42894	0.43358	0.26950	0.24809
1.0	1	0.0	0.61944	0.61457	0.50545	0.45217
		0.5	0.62974	0.62722	0.45367	0.42763
		1.0	0.64047	0.64052	0.39969	0.39625
	4	0.0	0.41829	0.42015	0.36465	0.33209
		0.5	0.42387	0.42675	0.32549	0.30127
		1.0	0.42994	0.43407	0.28341	0.26323

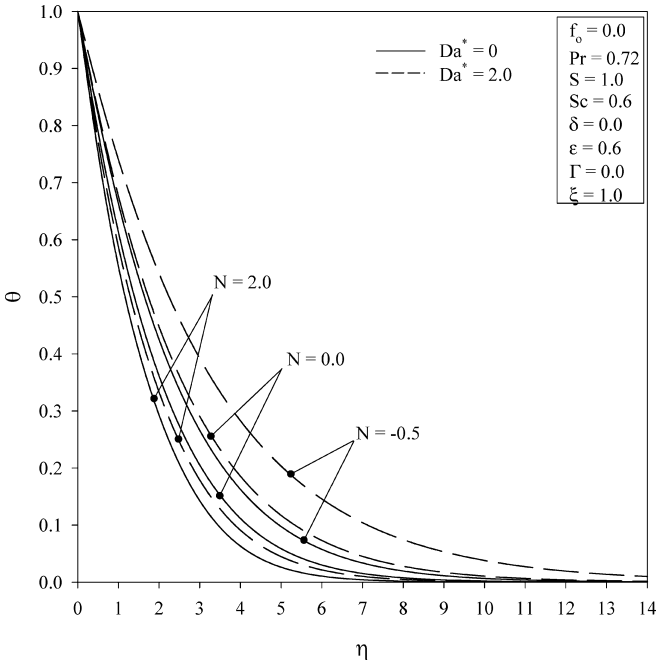

Fig. 2. Effects of Da* and N on the Temperature Profiles

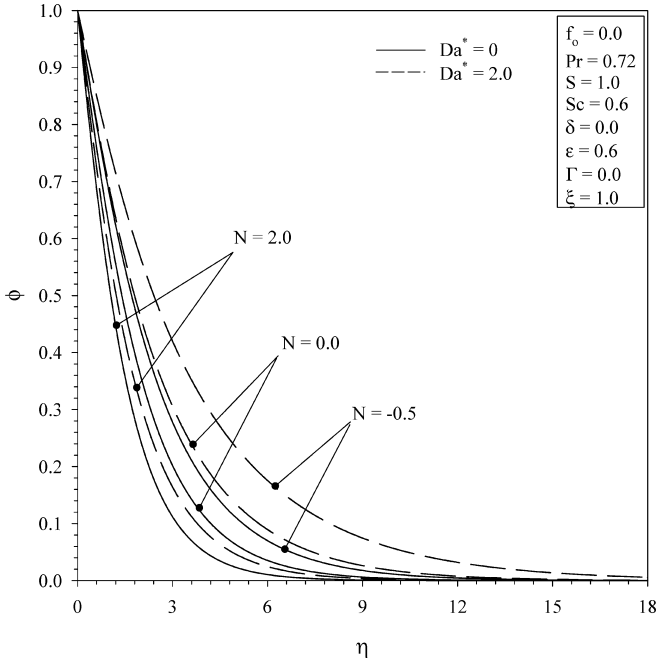

Fig. 3. Effects of Da* and N on the Concentration Profiles

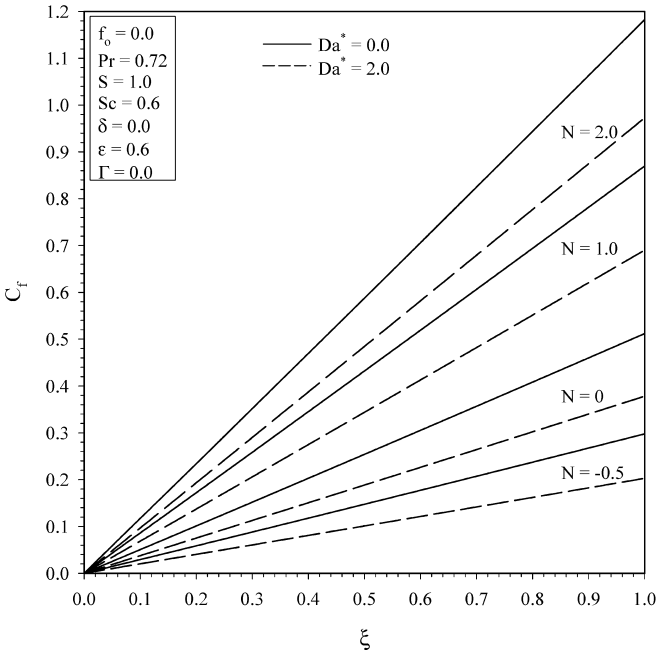

Fig. 4. Effects of N and Da* on the Skin-Friction Coefficient

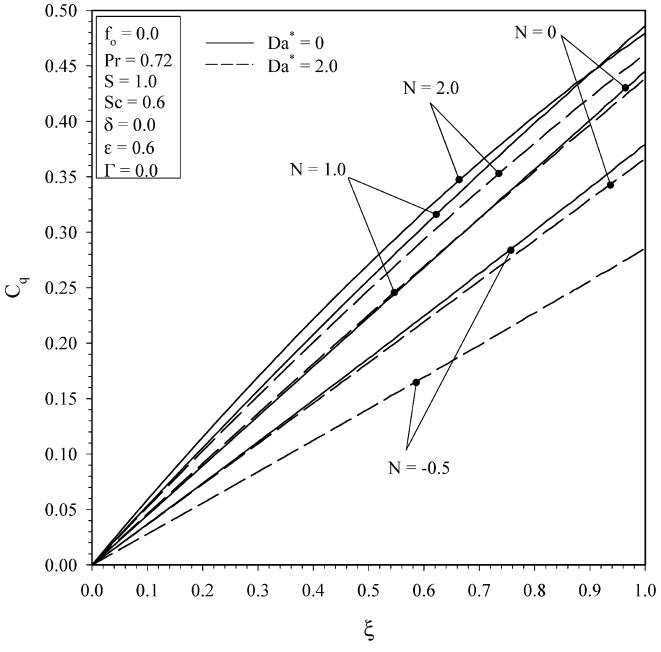

Fig. 5. Effects of N and Da* on the Wall Heat Transfer

porous medium. Obviously, all of C_f, C_q and C_m increase with increasing values of ξ since they are defined as directly proportional to ξ.

Figures 7 and 8 display the effects of the heat generation or absorption coefficient δ and the porous medium thermal dispersion parameter S on the velocity and temperature profiles at ξ = 1, respectively. The presence of heat generation effects (δ>0) has the tendency to increase the temperature of the fluid. This causes the buoyancy effects to increase for aiding flow (N>0) resulting in more induced flow along the surface. Both the hydrodynamic and thermal boundary layers tend to increase as δ increases. Also, for δ>0 a distinctive peak in the temperature profile occurs in the vicinity of the surface. The opposite effect is obtained due to the presence of heat absorption effects (δ<0). The peak temperature value occurs at the wall for this case. In general, the porous medium thermal dispersion effects increase the temperature of the fluid causing higher flow rates along the surface. However, it appears from Figures 7 and 8 that for δ = 1, the peak values of the temperature and velocity profiles are lowered as S increases.

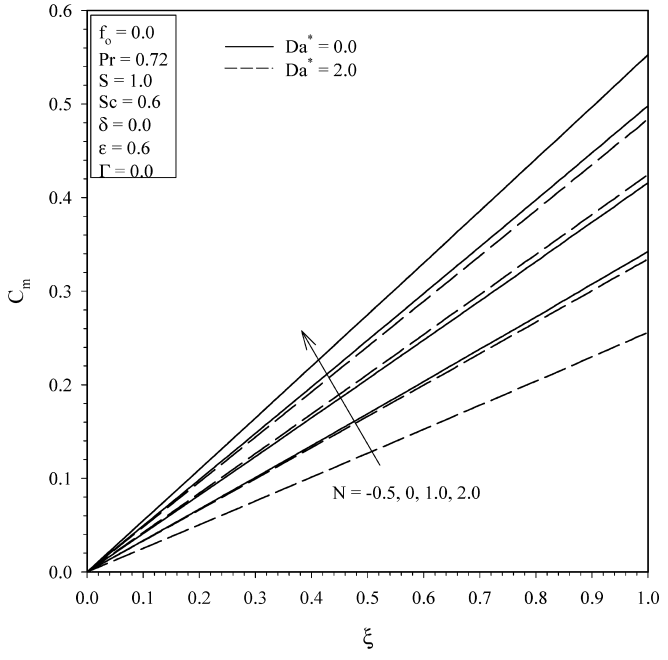

Fig. 6. Effects of N and Da* on the Wall Mass Transfer

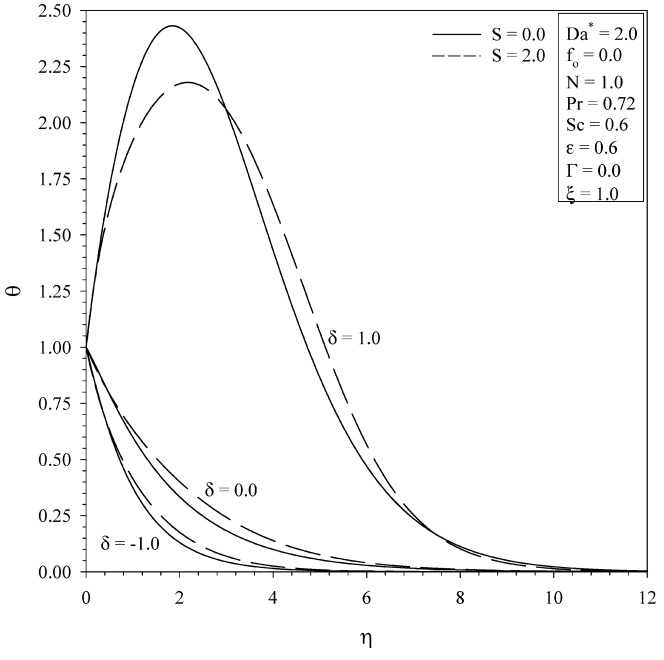

Fig. 8. Effects of S and δ on the Temperature Profiles

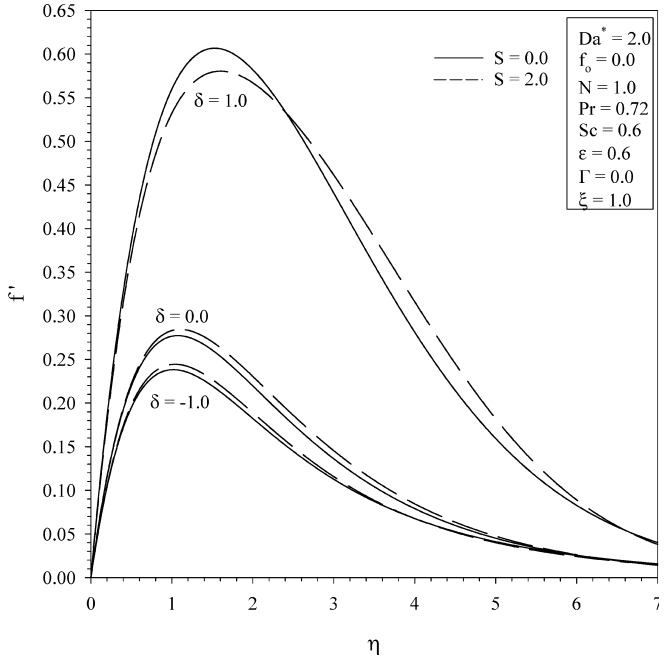

Fig. 7. Effects of S and δ on the Velocity Profiles

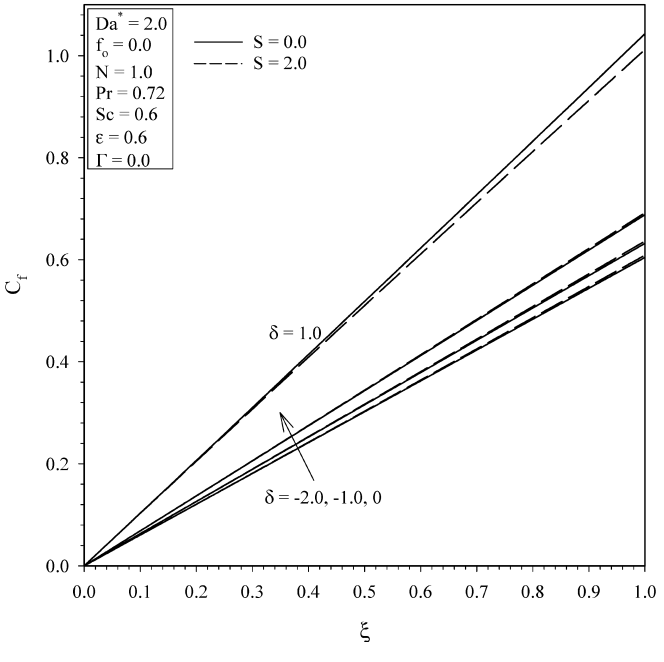

Fig. 9. Effects of S and δ on the Skin-Friction Coefficient

Figures 9 and 10 depict the influence of both S and δ on the values of C_f and C_q along the surface, respectively. It is predicted that increases in the porous medium thermal dispersion parameter S increase both C_f and C_q (except for $\delta = 1$). In addition, increases in the value of δ produce increases in the values of C_f and decreases in the values of C_q. It is also predicted that C_q becomes negative along the whole surface for $\delta = 1$. This is associated with the existence of the peak in the temperature profiles for $\delta = 1$ which causes its wall slope to change its sign.

Figures 11 and 12 present typical velocity and temperature profiles at $\xi = 1$ for various values of the wall mass transfer parameter f_o and the dimensionless porous medium inertia parameter Γ, respectively. Imposition of fluid wall suction (f_o>0) tends to decrease both the velocity and temperature of the fluid as well as their boundary-layer thicknesses. On the other hand, injection or blowing of fluid at the surface produces the exact opposite effect namely increases in the fluid velocity and temperature and their boundary-layer thicknesses. These behaviors are obvious from Figures 11 and 12. The presence of the porous medium inertia effects increases the resistance to flow. This causes the fluid velocity to decrease and its

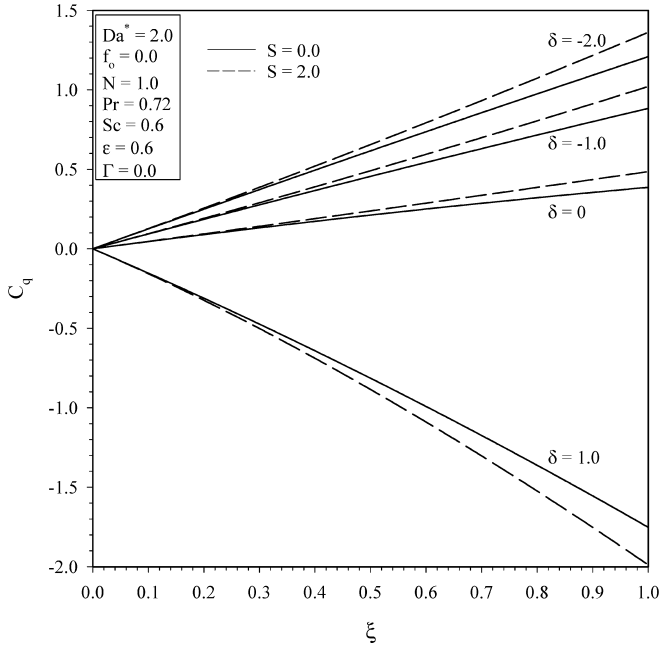

Fig. 10. Effects of S and δ on the Wall Heat Transfer

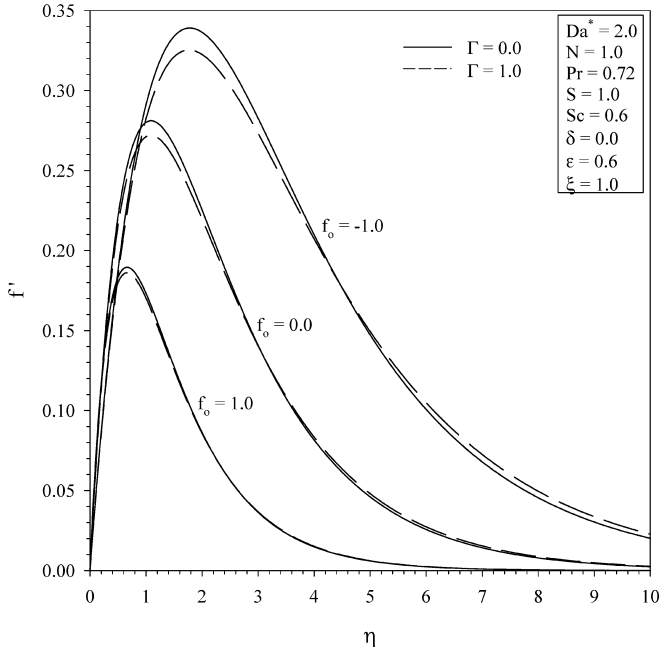

Fig. 11. Effects of f_0 and Γ on the Velocity Profiles

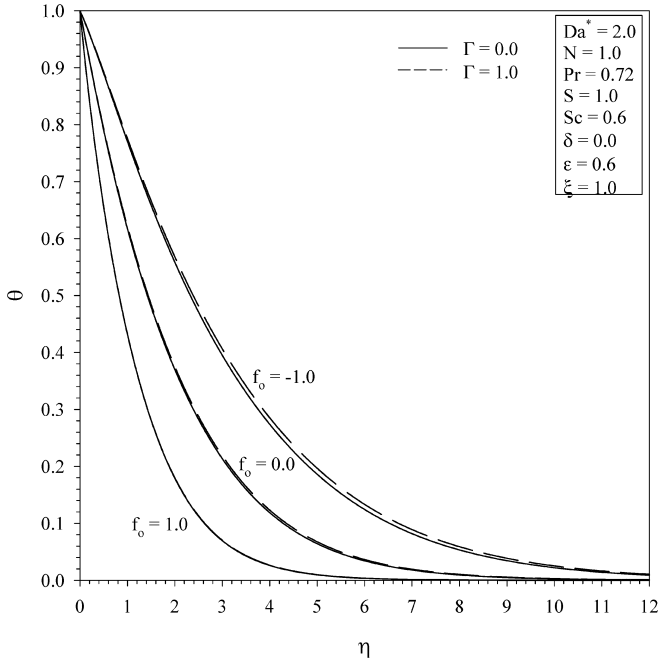

Fig. 12. Effects of Γand f_0 on the Temperature Profiles

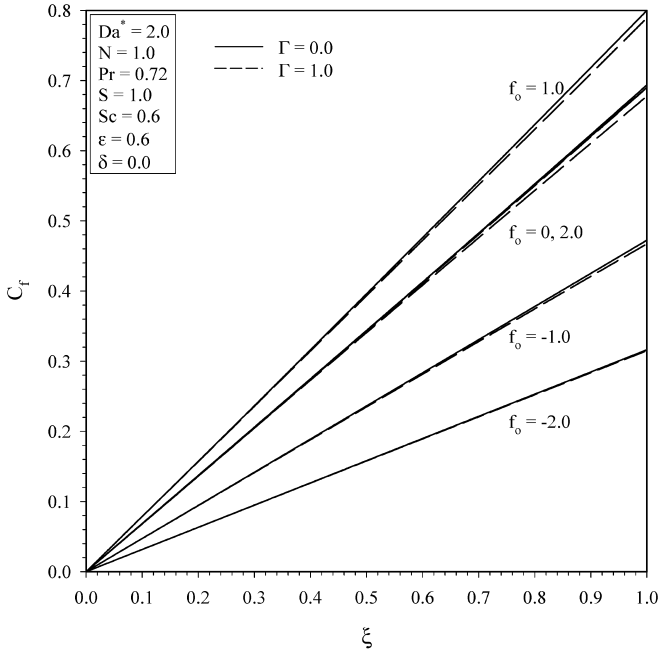

Fig. 13. Effects of f_0 and Γ on the Skin-Friction Coefficient

temperature to increase as obvious from Figures 11 and 12.

Figures 13 and 14 illustrate the effects of f_o and Γ on the distribution of C_f and C_q along the surface, respectively. It is predicted that imposition of fluid suction at the wall produces increases in both the skin-friction coefficient C_f and the wall heat transfer coefficient C_q. On the other hand, injection or blowing of fluid into the boundary layer from the plate surface causes reductions in both C_f and C_q. This is clear from Figures 13 and 14. In addition, these figures show that increases in the value of the porous medium inertia parameter Γ result in slight decreases in both C_f and C_q.

Figures 15 and 16 depict the influence of the wall mass transfer parameter f_o and the Schmidt number Sc on the concentration profile at $\xi = 1$ and the distribution of the wall mass transfer coefficient C_m along the surface, respectively. Similar to the temperature profiles, imposition of wall fluid suction ($f_o>0$) reduces the concentration and its boundary-layer thickness while application of wall fluid injection or blowing ($f_o<0$) increases them. In addition, increases in the value of the Schmidt number Sc results in decreases in the concentration level in the fluid. These behaviors are clear from Figure 15.

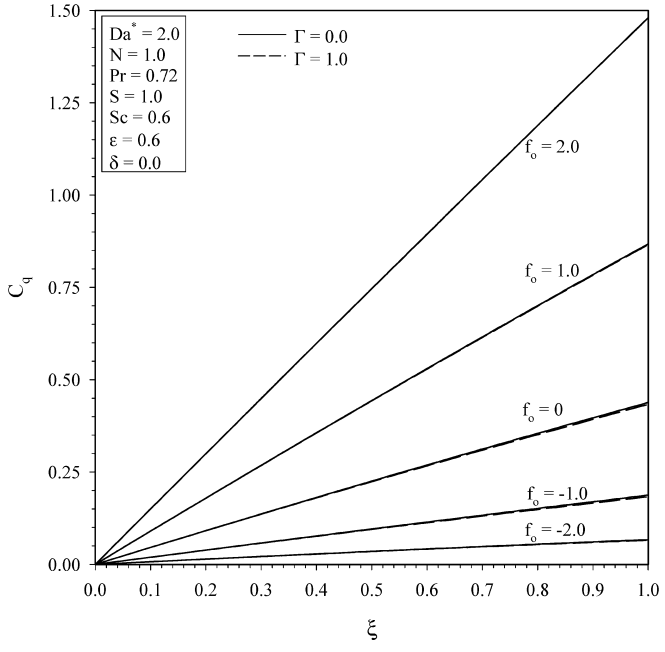

Fig. 14. Effects of f_o and Γ on the Wall Heat Transfer

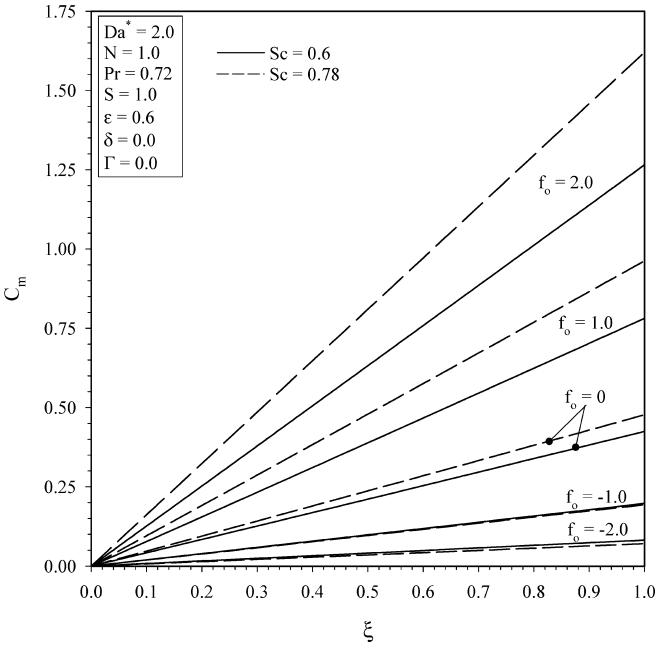

Fig. 16. Effects of f_0 and Sc on the Wall Mass Transfer

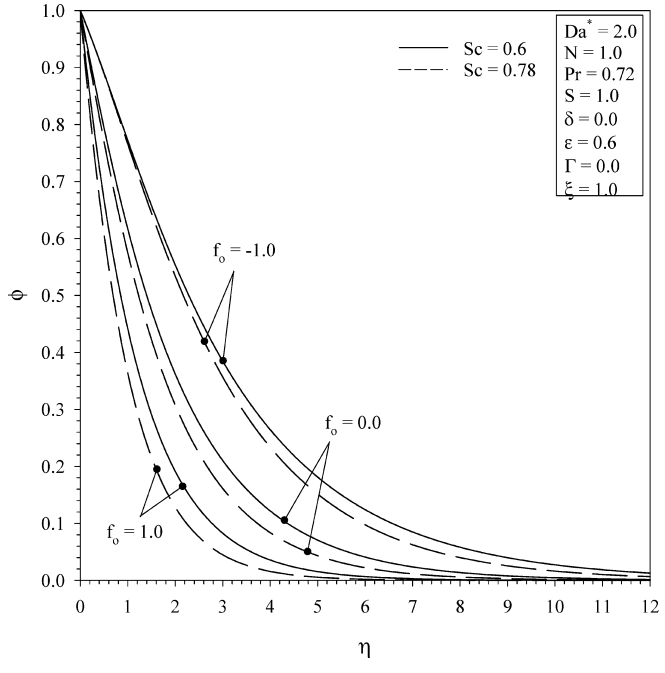

Fig. 15. Effects of f_0 and Sc on the Concentration profiles

Furthermore, increases in the amount of fluid wall suction increases the negative slope of the concentration profile for every location along the surface except at the leading edge. This causes the wall mass transfer coefficient C_m to increase. However, increases in the amount of injection reduce the values of C_m for every ξ value except $\xi = 0$. The effect of increasing the value of Sc is seen to increase the value of C_m for $f_o \geq 0$ and to decrease it for $f_o<0$. These facts are apparent from Figure 16.

5 Conclusion

The problem of steady, laminar, simultaneous heat and mass transfer by natural convection boundary-layer flow of a viscous, Newtonian and heat generating or absorbing fluid over a vertical permeable plate embedded in a uniform porous medium with inertia and thermal dispersion effects was considered. Both the wall temperature and concentration were assumed to vary linearly with the vertical distance along plate. The governing equations for this problem were developed and transformed using appropriate non-similarity transformations. The resulting transformed equations were then solved numerically by an implicit, iterative, finite-difference scheme. The obtained results for special cases of the problem were compared with previously published work and found to be in good agreement. It was found that, in general, the local skin-friction coefficient increased as either of the porous medium dispersion effects, buoyancy ratio, wall suction effects, or the heat generation effects increased and it decreased as a result of the presence of the porous medium, surface injection effects, or the heat absorption effects. In addition, the local heat transfer coefficient was predicted to increase due to increases in either of the porous medium thermal dispersion effects, buoyancy ratio, suction effects, or the heat absorption effects while it decreased as the inverse Darcy number or the wall injection effects increased. Furthermore, the local mass transfer coefficient was predicted to increase as a result of increasing either of the buoyancy ratio, the wall fluid suction or the Schmidt number for positive values of the wall mass transfer parameter while it decreased due to the presence of the porous medium. It is hoped that the present work will serve as a vehicle for understanding more complex problems involving the

various physical effects investigated in the present problem.

References

Acharya, S. and Goldstein, R.J., Natural Convection in an Externally Heated Vertical or Inclined Square Box Containing Internal Energy Sources, ASME. J. Heat Transfer, 1985, 107, 855–866

Amiri, A. and Vafai, K, Analysis of Dispersion Effects and Non-Thermal Equilibrium, Non-Darcian, Variable Porosity Incompressible Flow Through Porous Media, Int. J. Heat Mass Transfer, 1994, 37, 936–954

Bejan, A., Convection Heat Transfer, Wiley, New York, 1984

Bejan, A. and Khair, K.R., Heat and Mass Transfer by Natural Convection in a Porous Medium, Int. J. Heat Mass Transfer, 1985, 28, 909–918

Blottner, F.G., Finite-Difference Methods of Solution of the Boundary-Layer Equations, AIAA Journal, 1970, 8, 193–205

Chamkha, A.J., Non-Darcy Hydrodynamic Free Convection From a Cone and a Wedge in Porous Media, Int. Commun. Heat Mass Transfer, 1996, 23, 875–887

Chamkha, A.J., Non-Darcy Fully Developed Mixed Convection in a Porous Medium Channel with Heat Generation/Absorption and Hydromagnetic Effects, Numer. Heat Transfer, 1997, 32, 853–875

Cheng, P., Heat Transfer in Geothermal Systems, Advances in Heat Transfer, 1978, 4, 1–105

Cheng, P. and Minkowycz, W.J., Free Convection about a Vertical Flat Plate Embedded in a Porous Medium with Application to Heat Transfer from a Dike, J. of Geophy, 1977, 82, 2040–2044

Cheng, P. and Vortmeyer, D., Transverse Thermal Dispersion and Wall Channeling in a Packed Bed with Forced Convective Flow, Chemical Eng. Science, 1988, 43, 2523–2532

El-Hakiem, M.A., Viscous Dissipation Effects on MHD Free Convection Flow Over a Nonisothermal Surface in a Micropolar Fluid, Int. Comm. Heat Mass Transfer, 2000, 27, 581–590

Gorla, R.S, Bakir, A.Y and Byrd, L., Effects of Thermal Dispersion and Stratification on Combined Convection on a Vertical Surface Embedded in a Porous Medium, Transport in Porous Media, 1996, 25, 275–282

Hong, J., Yamada, Y., and Tien, C.L., Effect of non-Darcian and Nonuniform Porosity on Vertical-Plate Natural Convection in Porous Media, J. Heat Transfer, 1987, 109, 356–362

Hsu, C.T. and Cheng, P., Thermal Dispersion in a Porous Medium, Int. J. Heat Mass Transfer, 1990, 33, 1587–1597

Kim, S.J., and Vafai, K., Analysis of Natural Convection about a Vertical Plate Embedded in a Porous Medium, Int. J. Heat Mass Transfer, 1989, 32, 665–677

Lai, F.C., Coupled Heat and and Mass Transfer by Mixed Convection from a Vertical Plate in a Saturated Porous Medium, Int. Commun. Heat Mass Transfer, 1991, 18, 93–106

Lai, F.C. and Kulacki, F.A., Coupled Heat and Mass Transfer by Natural Convection from Vertical Surfaces in Porous Media, Int. J. Heat Mass Transfer, 1991, 34, 1189–1194

Nield, D.A., and Bejan, A., Convection in Porous Media, Springer, NewYork, 1992

Plumb, O.A., Thermal Dispersion in Porous Media Heat Transfer, ASME/JSME Thermal Conference Proceedings, 1983, 2, 17–21

Plumb O.A., and Huenefeld, J.C., Non-Darcy Natural Convection from Heated Surfaces in Saturated Porous Media, Int. J. Heat Mass Transfer, 1981, 24, 765–768

Raptis, A., Tzivanidis, G. and Kafousias, N., Fre Convection and Mass Transfer Flow through a Porous Medium Bounded by an Infinite Vertical Limiting Surface with Constant Suction, Lett. Heat Mass Transfer, 1981, 8, 417–424

Vafai, K. and Tien, C.L., Boundary and Inertia Effects on Flow and Heat Transfer in Porous Media, Int. J. Heat Mass Transfer, 1981, 24, 195–203

Vajravelu, K. and Nayfeh, J., Hydromagnetic Convection at a Cone and a Wedge, Int. Commun. Heat Mass Transfer, 1992, 19, 701–710

Yagi, S., Kunii, D. and Endo, K., Porous Medium Heat Transfer, Int. J. Heat Mass Transfer, 1985, 7, 333–339